RESEARCH PAPER

Experimental and Numerical Model of Interior Reinforced Concrete Beam–Column Joints Strengthened with Carbon Fiber-Reinforced Polymer Sheets

Shahriar Shahbazpanahi[1] · Farzad Hejazi[2] · Arash Rahimipour[2] · Masoud Paknahad[3]

Abstract

The present study involves full-scale experimental test and numerical model of interior reinforced concrete beam–column joints strengthened by carbon fiber-reinforced polymer (CFRP) sheets. The present study proposes a novel strengthening technique for interior beam–column joints. The experimental test intends to achieve a fundamental understanding of the behavior of interior joint strengthened by CFRP wrap in columns region with L-shape overlays on the top and bottom of beams. The purpose of implementing this system is to transfer the failure of the columns regions to the beams regions. This technic is a feasible economic solution. Hence, two beam column joints were made and tested. One interior joint was tested in an unstrengthened condition to act as the control joint. A numerical simulation based on plastic damage model by ABAQUS software was carried out to validate the experimental results. The CFRP wrap mechanism prevented the development of cracks in the joint. The length of cracks decreased because CFRP sheets were applied. The average decrease was approximately 37% of the crack length of the control beam–column joint. It is observed that the compression strut zone was increased by the application of CFRP wrap in the column zone.

Keywords Carbon fibre reinforced polymer · Beam-column joints · Strengthening · Reinforced concrete

1 Introduction

Beam–column joints provide resistance for applied external loads when the bending moment encounters the joint. One of the most important structural elements is the beam–column joint. A failure mode may happen in the joint region (shear failure), in the beam region (beam hinge) or in the column region. Shear failure in the joint region is more critical than other types of failure because it can break down the whole structure, and thus, it is crucial to strengthen a study of behavior, crack pattern and failure

mode. Failure can be moved to the adjacent beam region to prevent shear failure in the joint region (Shahbazpanahi et al. 2018). To avoid such failure, carbon fiber-reinforced polymer (CFRP) sheets can be utilized to strengthen beam–column joints. They are widely used in concrete due to their corrosion resistance, low weight, high tensile strength and large strain (Shahbazpanahi et al. 2013a, b; Bruno et al. 2017). They can improve the flexural capacity (Shahbazpanahi and Kamgar 2014) and the shear strengthening (Shahbazpanahi et al. 2014a, b). Indubitably, they can also help prevent the crack propagation (Shahbazpanahi et al. 2012; Shahbazpanahi and Kamgar 2014).

Many studies have adopted experimental tests and numerical and analytical methods to carry out CFRP-strengthened beam column joints. Alhaddad et al. (2012) focused on the response of beam column joints before and after the CFRP and textile-reinforced mortar (TRM) upgrade had taken place. Apart from that, Xiaobing et al. (2013) conducted experimental tests to examine the mechanical behavior of square FRP-strengthened beam column joints. There were nine RC beam column joints

✉ Farzad Hejazi
  farzad@fhejazi.com

[1] Department of Civil Engineering, Sanandaj Branch, Islamic Azad University, Sanandaj, Iran

[2] Department of Civil Engineering, Housing Research Centre, University Putra Malaysia, Serdang, Malaysia

[3] Faculty of Civil Engineering, Mahallat Institute of Higher Education, Mahallat, Iran

tested by Singh et al. (2013) under static loading. CFRP strengthening was carried out on beam column joints, where CFRP was placed in an L-shape at 45° in a two-layer joint. Moreover, Realfonzo et al. (2014) conducted experimental tests on eight full-scale beam column subassemblies. Seven of them were strengthened by different CFRP systems, but the last one was utilized as a benchmark. Del Vecchio et al. (2014) carried out experimental tests on six full-scale RC joints under constant axial load and CFRP-strengthened configuration. They compared the experimental capacities of the as-built joints in their experiment.

Bsisu and Hiari (2015) relied on CFRP and FEA to present an analytical investigation of a strengthening technique. Their research intended to improve the behavior of RC beam column joints in terms of their performance and load-carrying capacity of the structures. Then, Baji et al. (2015) developed a nonlinear finite element model to examine the effect of CFRP strengthening on RC beam column joints. Smeared crack elements were used in the numerical analysis. Baji et al. (2015) presented various numerical models of reinforced beam–column joints that were facilitated by CFRP. However, limited experimental studies have been done to look at how CFRP strengthens RC beam–column joints because of financial constraints.

Many investigations have confirmed the effectiveness of CFRP strengthening to prevent the shear failure of RC beam–column joints (Balaji and Thirugnanam 2017; Elshamandy et al. 2018; Santarsiero 2018). These studies also demonstrate a significant increase in the strength of the joints. However, economic considerations are disregarded to devise economical strengthening solution. In most previous systems, CFRP wrap was used in the beams or joint regions to create a slight confinement effect. In fact, few researches have emphasized on the use of CFRP wraps as a strengthening solution in columns (Fig. 1), which is likely
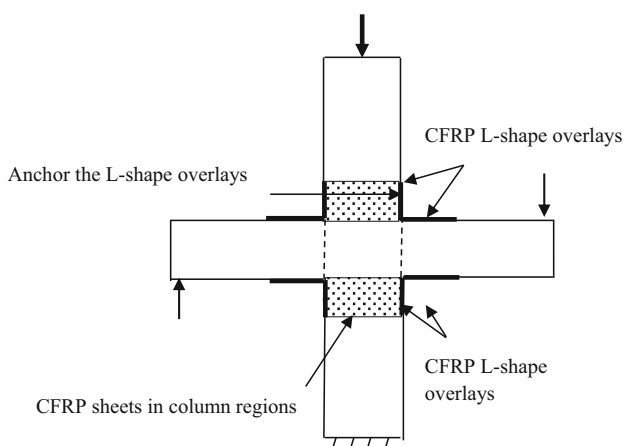
to create a different failure mode, for example, beam failure.

The experimental test would like to achieve a fundamental understanding of the behavior and failure mode of the joint, strengthened by CFRP sheets in column regions with an L-shape overlay on the beams. This system is expected to influence the economical design of the joint in order to transfer the failure of the column regions to the beams. The purpose of this scheme is to anchor the CFRP L-shape overlays on the top and bottom of the beams (Fig. 1). To make it happen, two interior beam–column joints were made and tested. One interior joint was particularly tested in an unstrengthened condition to act as a control joint. Employing ABAQUS software, a numerical simulation based on plastic damage model is carried out to validate the results.

2 Methodology

2.1 Experimental Specimens and Test Setup

The authors conducted comprehensive experimental tests for joint specimens to identify the behavior of joint, strengthened by CFRP sheets, in column regions with an L-shape overlays on the top and bottom of the beams.

2.1.1 Specimens

The experiment comprised two full-scale interior beam column joint specimens subjected to static monotonic load. The beam column joints were built and tested in a structural engineering laboratory at Universiti Putra Malaysia. The two-way interior beam column joint is complex because of the possible two-way action in the frame structure as compared with the current knowledge about joint behavior (Deaton 2013). One of the specimens was the control beam column joint, whereas another specimen was strengthened by CFRP sheets solely in column regions with L-shape overlays on the beams. The specimens were designed according to the ACI 318-63 code. The column was held in place by the bottom hinges. The position was fixed by a support frame. The column was 2,700 mm high with a cross-section dimension of 400 mm × 400 mm. The length of the beam was 1,800 mm from the face of the column with a cross-section of 300 mm × 300 mm. The columns were reinforced by eight steel bars measuring 25 mm in diameter. Transverse shear reinforcements with a diameter of 10 mm were provided in the columns.

The column stirrups were spaced at 170 mm in the joint and 600 mm above and below the joint. The two top longitudinal reinforcements of the beams were 25 mm in diameter. In contrast, the bottom longitudinal

Fig. 1 Anchor the CFRP L-shape overlays by CFRP sheets in column regions

reinforcements were two pieces of bars with a diameter of 20 mm. The stirrup reinforcement of the beam was a rectangular tie with a diameter of 8 mm starting from the face of the column.

Figure 2a shows the locations of the control joint strain gauges for specimen. The yield strengths of reinforcement steel bars and ties were 400 MPa. The mixing and specimen preparations are as follows. The water to binder ratio (W/b) is 0.4. Portland cement type 1 with the grade of 31.5 is used. The aggregates were washed, dried and then they were sieved and graded. The maximum size of coarse aggregate is 12.5 mm with specific gravity of 2.40. The fine aggregates are natural river sand with specific gravity of 2.64 and nominal maximum sizes of 4.7 mm. The aggregates grading is illustrated in Table 1.

The fine and coarse aggregates are mixed for 2 min in a drum mixer. Then, the cement is added. In the next step half of the premixed water is added and the mixture continues to blend for 1 min. The other remaining premix of water is added for 2 min. Then, the drum mixer is rotated for another 2 min. Samples are of 100 mm × 200 mm cylinders for compressive strength test. All samples are covered by plastic sheets followed by wet burlap for 24 h. The temperature in the laboratory is 30 °C with 50% relative humidity. An average of five samples results is used to find the compressive strength of samples according to ASTM C39. Based on the result of a standard cylinder, the strength of the concrete compressive was 21.5 MPa.

Figure 2b shows the details of the CFRP joint for specimens. The joint is strengthened by seven layers of CFRP wraps with 1.17 mm thickness in the column joint. The CFRP sheets are applied as L-shaped on the top and bottom surface of the concrete. Then, CFRP wraps were applied around the column at 150 mm above and below joint core. Ultimate tensile strength was 3800 MPa, tensile modulus was 240 GPa, and ultimate rupture strain was 1.55%. The length of these CFRP sheets was kept constant up to 600 mm. Due to imposition of point load, two steel plates at the top of the right side beam and bottom of the left side beam are located to apply incremental point load to the beam and avoid local damage.

2.1.2 Instrumentation

All instrument readings were set to zero including load cells, displacement transducers, and strain gauges. The specimens were in their initial undeformed position. They were used to monitor: (1) strains in all columns and beam bars on both the column-joint and beam-joint interfaces, (2) column axial load via load cells, (3) application of the
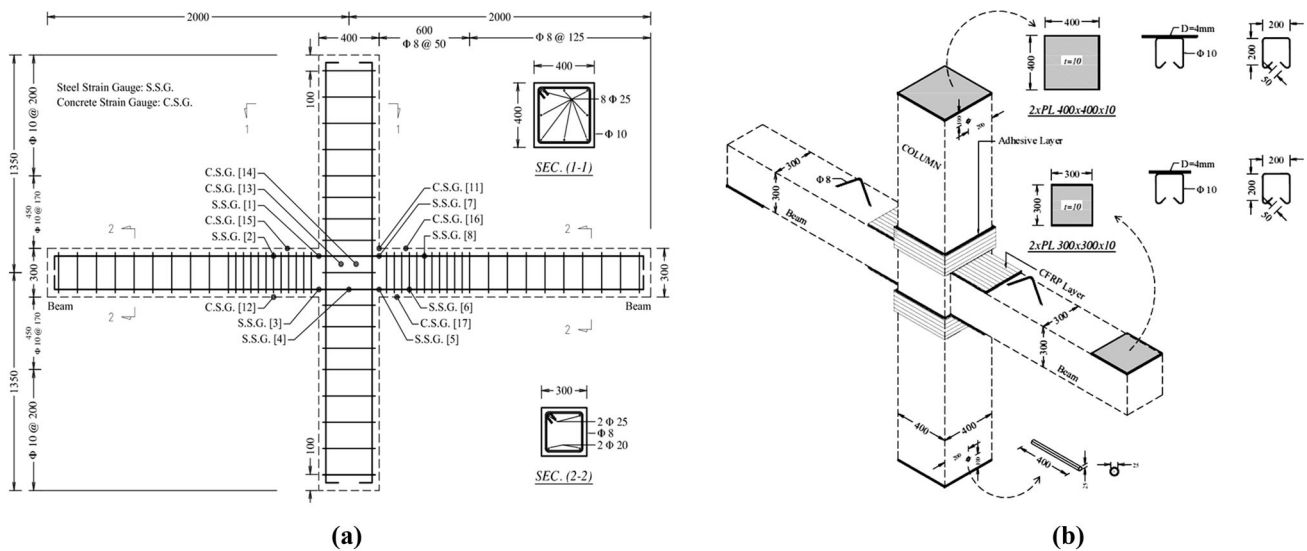

(a)   **(b)**

Fig. 2 Details of joint reinforcement and strengthened with CFRP. **a** Strain gauges locations, **b** joint strengthened with CFRP

Table 1 Aggregates gradation

	Sieve size								
	12.5 (mm)	9.5 (mm)	4.75 (mm)	2.36 (mm)	1.18 (mm)	600 (μm)	300 (μm)	150 (μm)	Pan
% Remained	0%	8%	32%	13%	11%	11%	10%	11%	3%

loads to the tips of the beams via two load cells, and (4) four LVDTs to measure displacement in different locations on the specimens (Fig. 3). Two LVDTs were used to measure the displacements of beam tips, whereas the rest were used to measure the rigid body motion of the joint. Electrical resistance strain gauges were employed to extract strains in the reinforcing steel and concrete in different locations. The strains were bonded to the steel bars in pre-grounded locations for smooth contact.

2.1.3 Test Setup and Procedure

Figure 4 shows the details of the test setup of joint, strengthened by CFRP wrap, in columns region with a L-shape overlaying on the top and bottom of the beams (behind view). Figure 5a portrays the details of the test setup for control joint, while Fig. 5b portrays the joint that was strengthened by CFRP. The joint specimen was tested under the constant application of axial load to the column (Fig. 5c). This load was considered the service load carried by the column under normal loading conditions. Then, two equal forces were applied to the end of the beam (Fig. 5d) to simulate the effect of gravity load design and two-way interior beam column joint. A load cell was used to measure the applied load. To simulate the inflection points at the centers of the upper and lower columns, one column was free to ensure that its ends could be freely rotated. To fulfill this purpose, the end of the column was supported by a link to extend from the strong floor directly and simulate hinge support. Then, a roller support was provided at the top of the column. The roller support was created in a 20 mm vertical slot. The test was conducted under an


Fig. 4 Joint strengthened by CFRP wrap in columns region with L-shape overlays on the top and bottom of beams (Behind view)

increasing monotonic load until the beam failure was reached. A constant axial load was applied on the top of the column using a static actuator. The applied column axial load specimens were kept constant at 150 kN, but the loads on the beam tips gradually increased starting from zero. Then, the corresponding displacements and strains were measured.
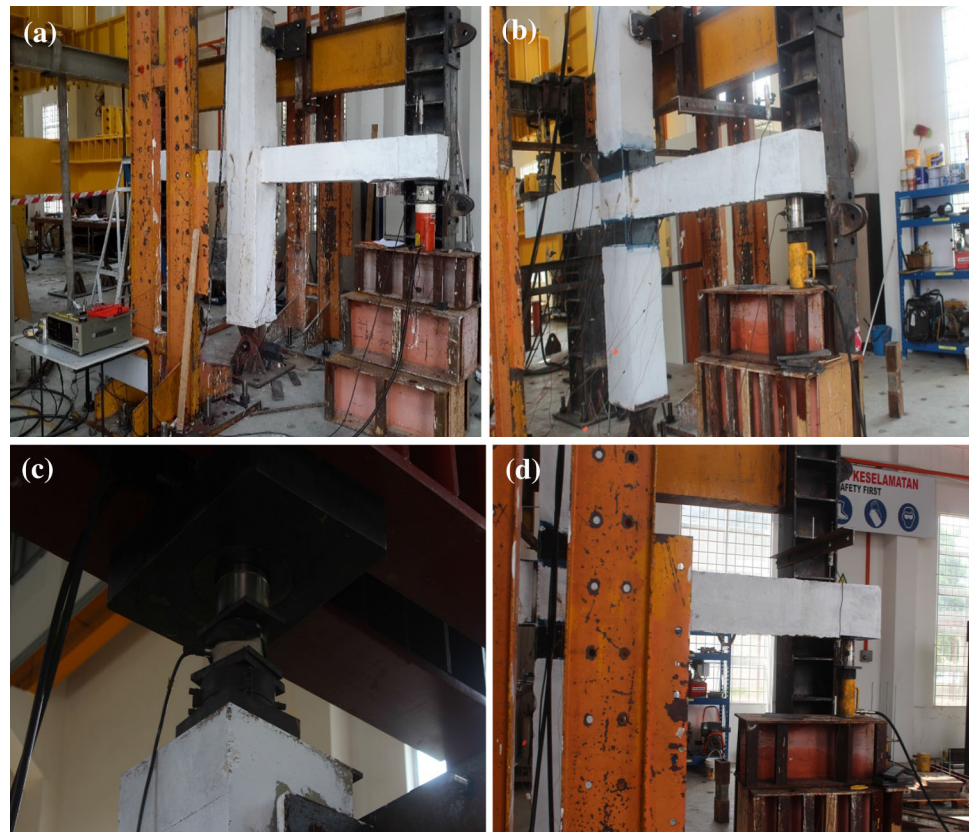
2.2 Finite Element Analysis

The 3D finite element model of the beams, developed by ABAQUS software, was employed to model the joints.

Fig. 3 Instrumentation and loading of specimen in testing
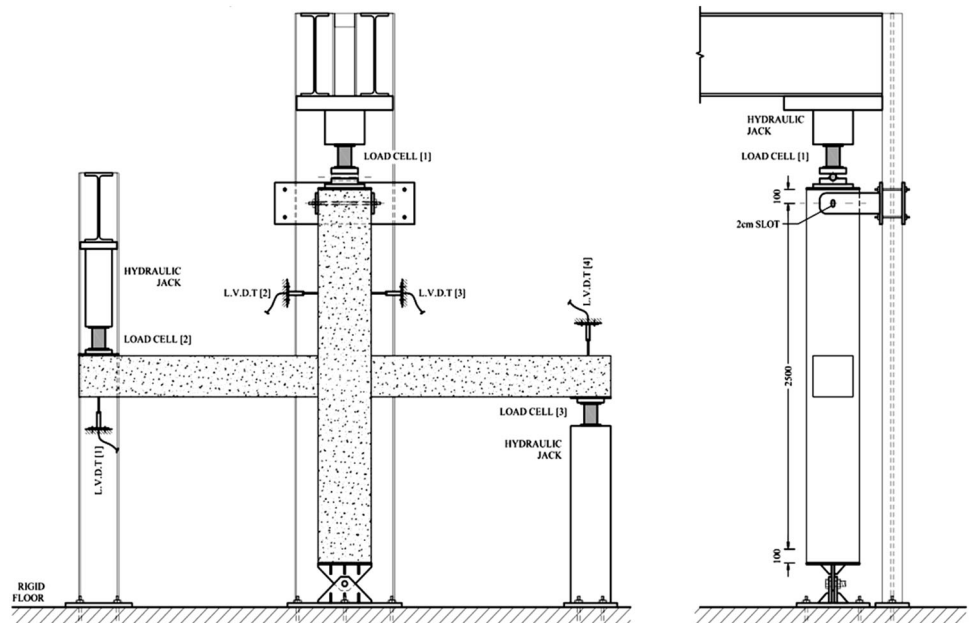
Fig. 5 Details of the test setup and applied loads. **a** The test setup for control joint, **b** test setup of strengthened joint, **c** load cell for axial load, **d** load cell for beams end

Plastic damage model was used to model the concrete behavior for both the column and beam. Tensile and compressive cracking were also expected in this model. Embedded region modeled the bond slip of reinforcement rebar steel. The concrete was simulated by a solid element with eight nodes with three degrees of freedom at each node. The concrete solid element is C3D8R in the ABAQUS model. The concrete behavior was considered as plastic and a homogeneous material. Reinforcement steel encircled in concrete in software embedded region must be selected for a truss element. Steel bar is defined as truss elements with 2 nodes and 3 translation freedom degree for each node. Truss element modeling in ABAQUS is called T3D2. This option was responsible for the degree of freedom for reinforcement bar because a slave element in concrete was selected as a host element. The reinforcement steels behavior was considered as elastic-perfect plastic. Bonding between reinforcement bar and concrete is assumed to be perfect. Three forces are applied to all cross-section one axial load to column which is set as pressure load in step in ABAQUS and two forces to beams with inverse position form up and down, both of which are defined as pressure force like columns force in step. The flowchart of the experimental and numerical analysis is shown in Fig. 6.

Four nodes shell elements, known as S4R, were used to model CFRP. The CFRP had linear elastic behavior. CFRP rupture was controlled by the CFRP tensile strength. The stress-slip between CFRP and the concrete was modeled by the approach from Nakaba et al. (2001). An eight-node interface element for transferring shear in nodal forces is applied between the concrete and FRP elements (Shahbazpanahi et al. 2014a, b).

The joint was modeled by ABAQUS FEA software with 10,985 within control joint using C3DBR elements (average size was 12 mm × 12 mm × 10 mm). Figure 7a depicts the assemblage reinforcement, whereas Fig. 7b depicts the hook and mesh in the ABAQUS software. The CFRP sheet was set at certain specific positions to strengthen the joints (Fig. 8).

3 Results and Discussion

This section presents the validation and comparison of results from the experimental and ABAQUS software. The results of the experimental and ABAQUS software discuss both the control beam–column joint and CFRP-strengthened joint.
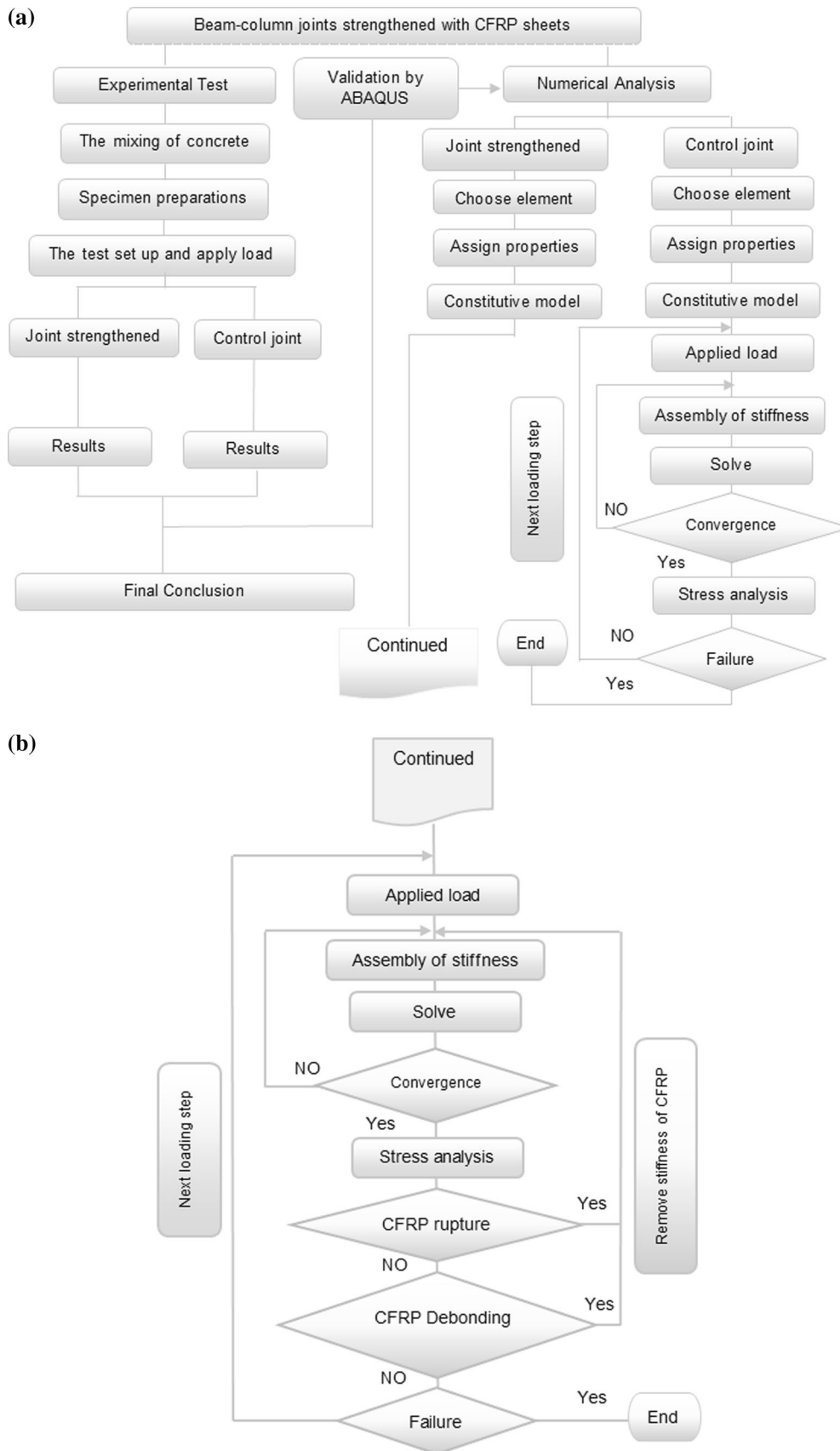
(a)

(b)

Fig. 6 Flowchart of the experimental and numerical analysis

3.1 Control Joint

Control joint is tested in Sect. 2.1. The load–displacement curves at the end of the beam obtained for control joint are compared with the result of the ABAQUS software, as shown in Fig. 9. The results of the experimental results are consistent with the result of the ABAQUS software. Failure load in the experimental results was predicted within 12% to 16% margin of error compared with the ABAQUS software based on plastic damage model. The load–displacement curves in the experimental results were similar to the ABAQUS software. The curve in the ABAQUS software was over-predicted. The curve shows that the load increased linearly until it reached 50 kN. Nonlinearity is initiated afterward. In the nonlinear part of the curve, the specimen reached a maximum load equal to 320 kN with 15 mm displacement at the end of the beams. The elastic stage is due to concrete cracking in the tension zone of the beams. The plastic stage is due to yielding of the beam longitudinal reinforcement.
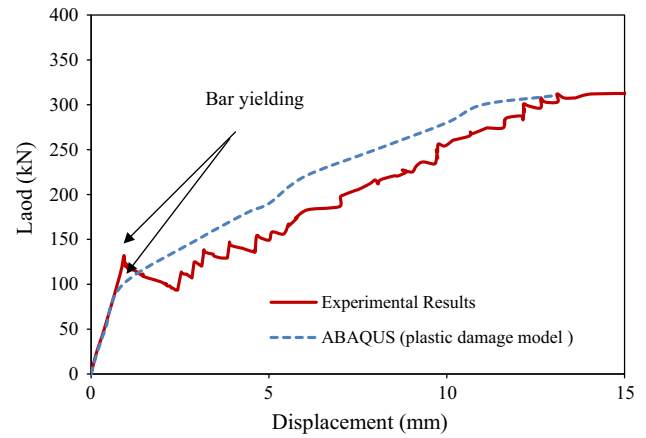

Fig. 9 Comparison of load–displacement curve for control joint

Figure 10a shows the hairline cracks observed from the experiment results at 170 kN load. The cracks patterns observed from the experiments and concrete principal

Fig. 7 Modeling of joint by ABAQUS software. **a** Bars position, **b** Mesh
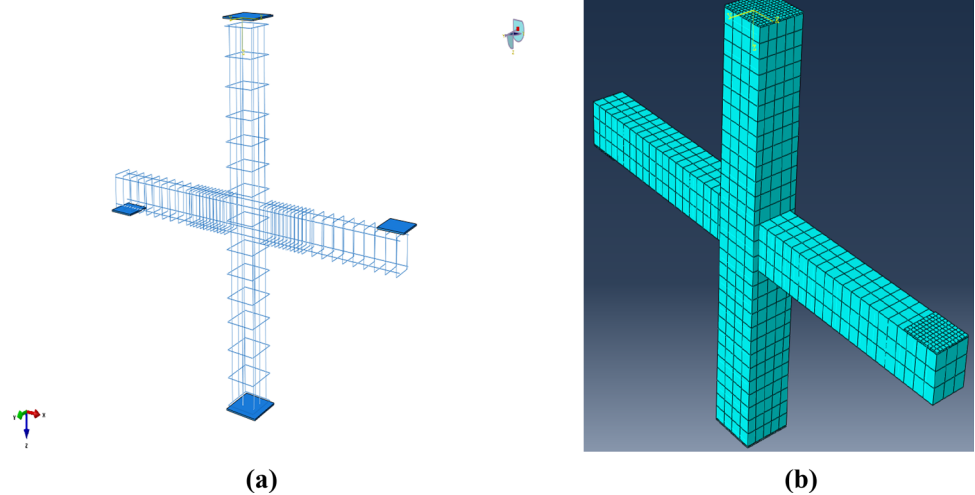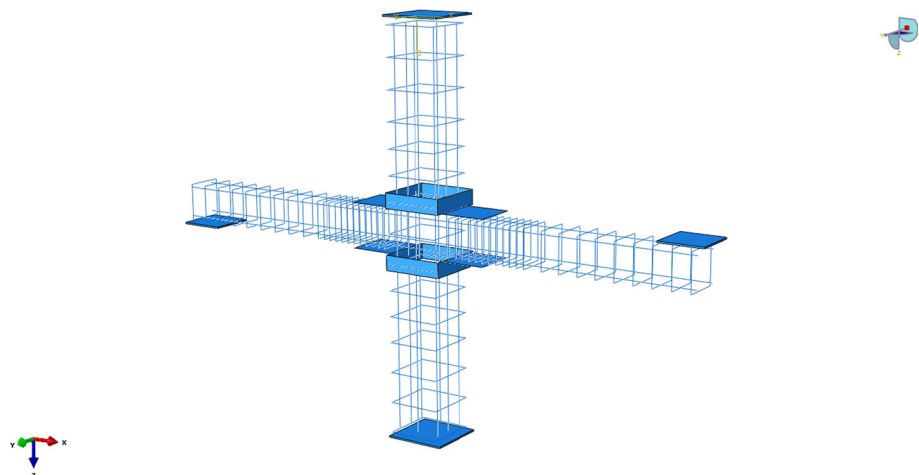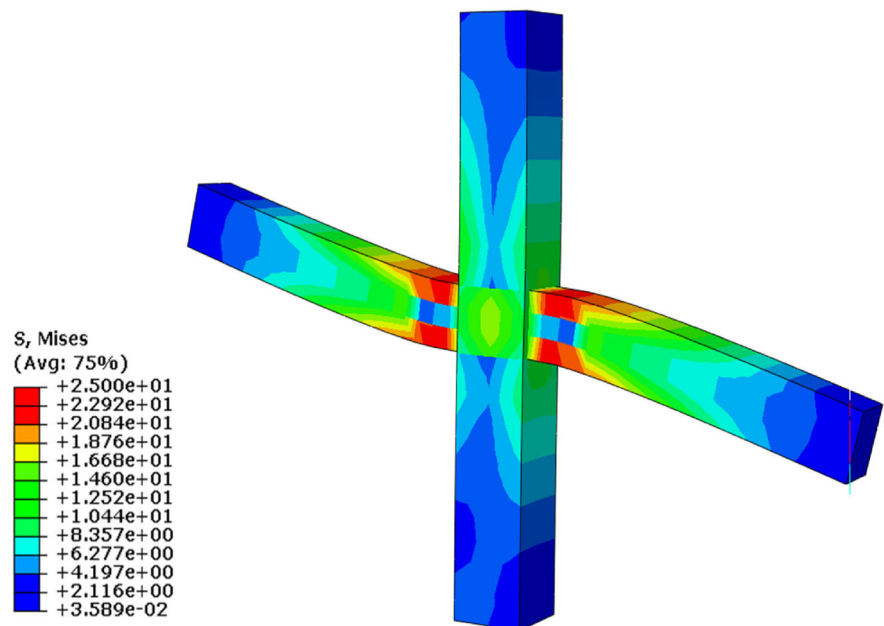

(a)

(b)

Fig. 8 Assembling bars, CFRP and plates

Fig. 10 Crack patterns in the control joint at 170 kN. **a** Crack patterns in the test. **b** ABAQUS software

(a)

(b)

stresses in the simulations are similar. Figure 10a shows the initial flexural crack at the beam bottom adjacent to the column faces. As the load increases, the beams show a second series of cracks that correspond to the stirrup position. The cracks open further at 170 kN. These distinct cracks extend through the depth of the beam section. Many smaller cracks formed along the beam. A major shear crack occurred and extended diagonally from the beam through the joint region. The experimental test predicted eight cracks within the beams.

In Fig. 10b, the concrete principal stresses obtained by ABAQUS software at 170 kN load are presented. A number of cracks may be too small to be seen in the real test. Based on the test results, control joint failed because of the yielding of the tension steel bars of the beam. Yield load occurred at approximately 250 kN. The numerical

results show that control joint failed because of the yielding of steel bars.

According to the test results, the behavior of the control joint after the yield load is slightly more ductile than the numerical results. The average values of parameters that characterize the stress–strain curves are listed in Table 2. The experimental joint test results show good agreement with ABAQUS software results. The maximum bar strain, displacement, and moment in the experiments and in ABAQUS software model are similar (12% to 18% error).

Figure 11 illustrates a diagonal compression strut. The concrete contribution to the joint shear resistance, caused by a strut action, accounts for the significant axial force in the column. The joint capacity could be limited by the failure of the diagonal strut. The major flexural crack in the beam and several cracks were formed in the column face (see Fig. 11).

A diagonal compression strut is illustrated in Fig. 13. The concrete contribution to the joint shear resistance, resulting from strut action, is accounted for only if the axial force in the column is significant. The joint capacity could be limited by the failure of the diagonal strut (Akguzel and Pampanin 2012). The major flexural crack in the beam and

several cracks formed in the column face is observed in Fig. 13. The maximum width of these cracks is 1.3 mm. Damage patterns in the control joint obtained by BAQUS software is shown in Fig. 14.

The maximum width of these cracks is 1.3 mm. Figure 12 shows the damage patterns in the control joint obtained by ABAQUS software.
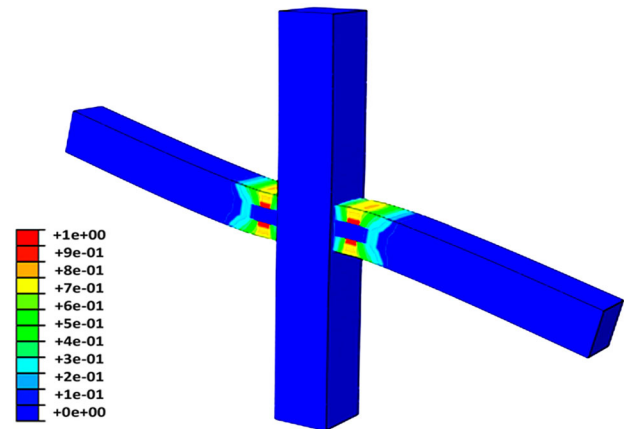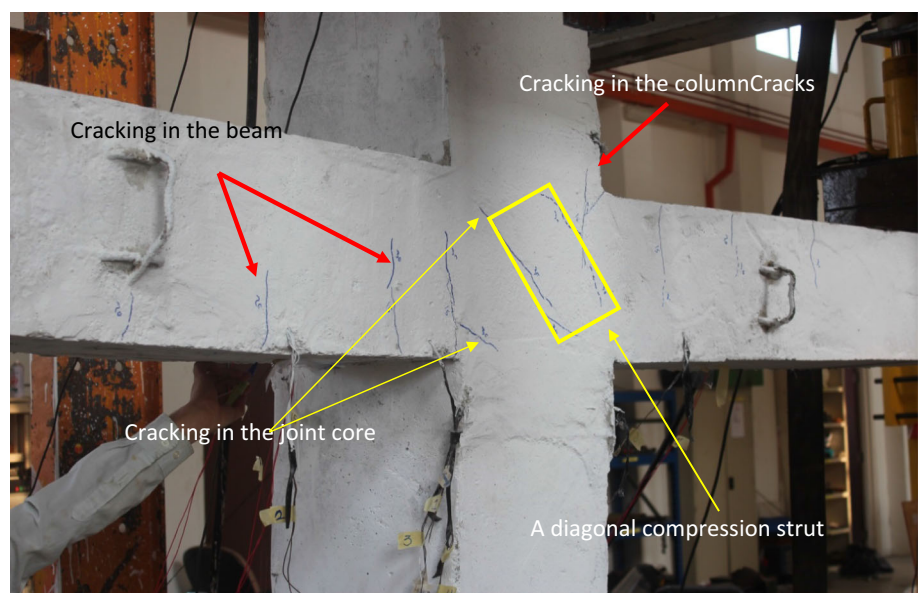

Fig. 12 Damage patterns in the control joint obtained by ABAQUS software

Table 2 Summary of test results and the ABAQUS software

|	Max bar strain		Δ_{max} (mm)	M_{max} (kN m)	θ_{max} (rad)
	Column face	Beam			
Experimental	2.64E−03	2.64E−2	15.6	56.02	0.00621
ABAQUS	2.56E−03	2.32E−1	14.5	56.27	0.0054

**Fig. 11** Crack patterns in the control joint at failure load (Behind view)

3.2 CFRP-Strengthened Joint

Figure 13 illustrates the comparison of results from load–displacement curve of the experimental test and ABAQUS software. The load–displacement result of the joint obtained by ABAQUS software was over-predicted as compared with the present experimental observation (14% to 20%). The load–displacement curve was divided into four parts: (1) linear elastic part (2) bar yielding of the beam longitudinal reinforcement (2) nonlinear plastic as a result of significant concrete cracking in the tension zone and small cracks in the joint region (3) an increase in the slope of the curve due to the effect of the CFRP wrap in columns region with L-shape overlays (4) debonding of L-shape overlays and rupture of the CFRP wrap (Fig. 13). The test results indicated that strengthening technique using CFRP sheets could improve the ductility of the beam–column joint.

Figure 14 illustrates the load–displacement curve based on the finite element analysis with different meshes. Mesh (a) had 1023 elements (element average size is 16 mm ×
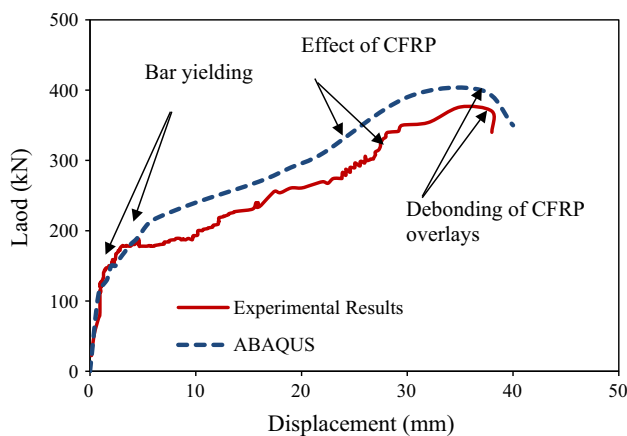
Fig. 13 Comparison of load–displacement curve for joint strengthened by CFRP
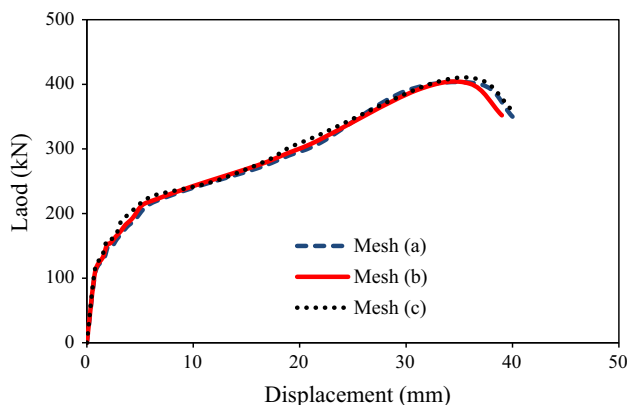
Fig. 14 Comparison between load–displacement curves for three meshes

16 mm × 15 mm) and 324 interface elements. Mesh (b) had 1726 elements (element average size is 14 mm × 14 mm × 12 mm) and 508 interface elements. Mesh (c) had 2862 elements (element average size is 10 mm × 8 mm × 8 mm) and 972 interface elements. The approximate matching of the three curves demonstrates the independence of the model from mesh size.

Figure 15 shows the cracks pattern of the joint in the experimental test at failure load. The figure shows several flexural cracks appeared around the CFRP sheet at the beam. Flexural cracks were observed on the top half of both beams between 1450 mm and 280 mm from the beam–column interface at 9 mm displacement. Additional cracking was also observed at 15 mm displacement. As the load increased, the initial flexural cracks started to propagate upward in the right and left of the beam. Major flexural cracks propagated into the upper half of the beams and the load increased (Shahbazpanahi et al. 2013a, b). The major cracks near the CFRP extended to one third of the beam below the compression face when the load was 270 kN. A small diagonal shear crack was observed in the joint region (Fig. 15). It was observed that debonding occurred between interfaces of the CFRP L-shapes overlay joint at failure load. Furthermore, this CFRP wrap mechanism prevented the development of cracks in the joint region. Then, retrofit shifted failure to the beam. To compare Figs. 11 and 15, the beam–column joint strengthened by CFRP significantly increased the ultimate load and deformation. The results showed that the beam–column joint achieved a higher ultimate force than control joint, which was highly flexible. At the same time, CFRP sheets dissipated the energy effectively. The use of CFRP prevented cracks in order to maintain the original shape of beam–column joint and increase deformability. The result showed that the CFRP sheets could delay crack propagations and reduce the lengths of cracks in the joint region. Figure 16 illustrates the displacement in the ABAQUS FEA software. Given the implementation of the CFRP sheets in the joint, no crack was observed on the surface of the column. The length of cracks decreased because CFRP sheets were applied. The average decrease was approximately 37% of the crack length of the control beam–column joint. The crack pattern obtained by the ABAQUS software predicted only one crack around CFRP. Crack propagation was controlled by CFRP sheets in the beam.

Figure 17 describes the debonding of the CFRP L-shapes overlays sheets and rupture of the CFRP wrap. A diagonal hairline crack appeared at the joint region. The width of this diagonal crack was 0.08 mm. The compression strut can also be seen in the figure. To compare Figs. 11 and 17, the width of the compression strut zone was increased by the application of CFRP wrap in the column zone.

Fig. 15 Crack pattern of the joint observed in experimental test
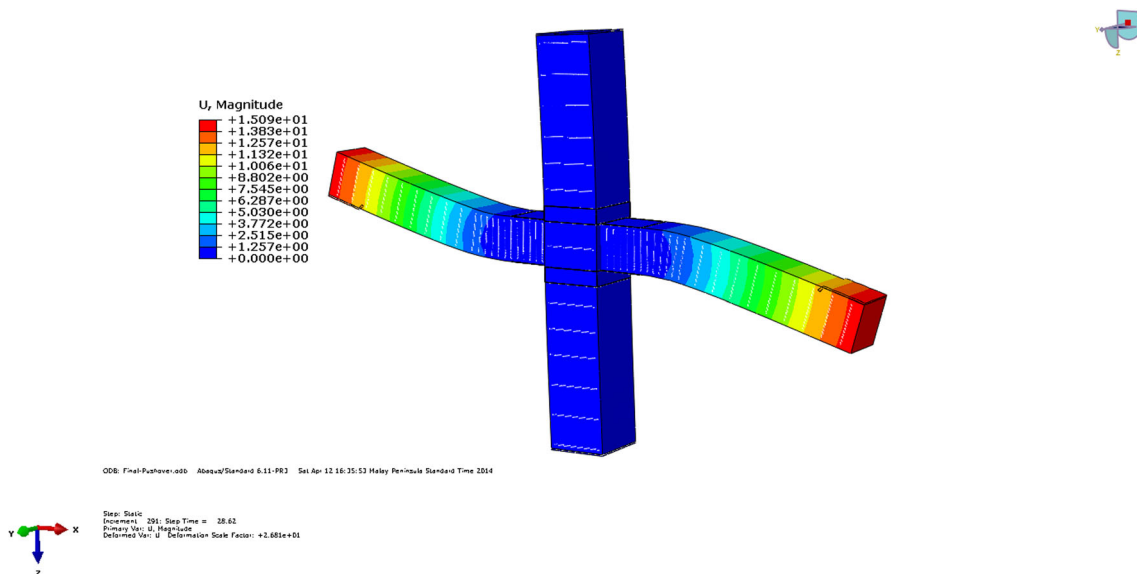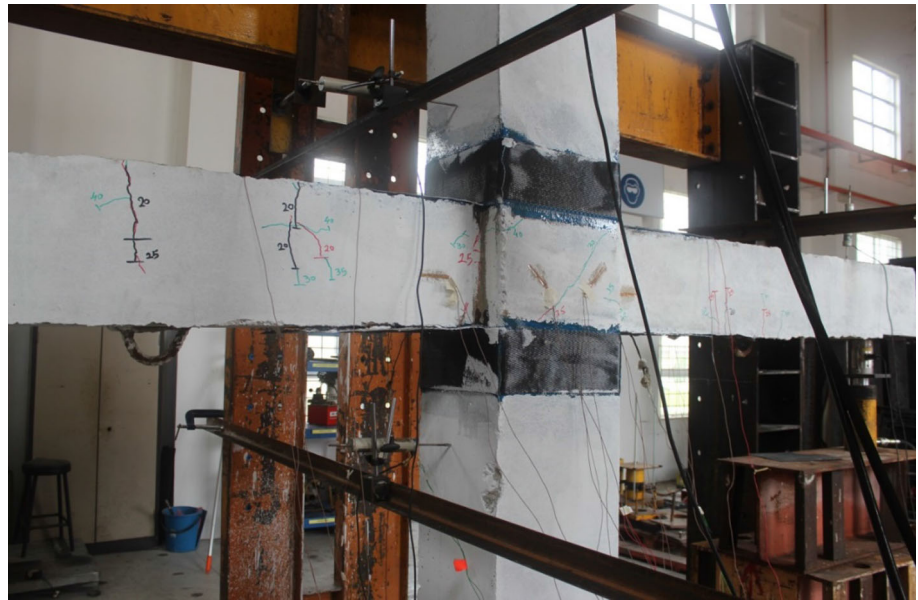
**Fig. 16** Crack pattern for joint obtained by ABAQUS software

Figure 18a shows the stress observed in the interior joint strengthened by CFRP. Stress represents the crack propagation that existed around the beams (Rahimipour et al. 2016). The majority of the stress is placed at the upper-right and bottom-left of the joint corners. This was because the unreasonable joint turn was the fundamental reason for the CFRP debonding in these areas. Figure 18b depicts stresses in the reinforcement bar reached 600 MPa.

Figure 19 shows the stresses in the CFRP wraps and L-shape overlay. The last strength of CFRP reached 3245 MPa. The rapture of the CFRP wraps was the final stage of the analysis, it occurs in Fig. 18 as well.

In this study, the benefit of the considered joint comparing the obtained results with other construction joints is to transfer the failure of the columns regions to the beams. To do so, the interior beam–column joints (Fig. 20) with other construction CFRP sheets, which were previously tested by Esmaeeli et al. (2015), are modeled to verify the benefit of the considered joint. Both joints are subject to the same boundary conditions. Figure 20 shows the predicted crack path in the joint modeled by the FEA software ABAQUS. It is interesting to observe that in the study reported by Esmaeeli et al. (2015), the crack path and the failure mechanism occurred in the joint region. In this

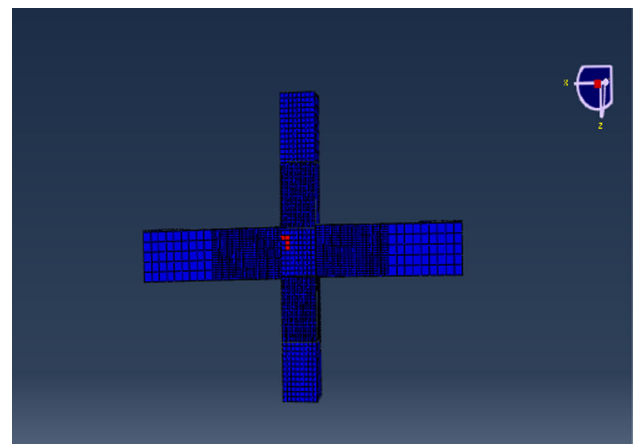**Fig. 17** Debonding in the CFRP L-shapes overlays in experimental test
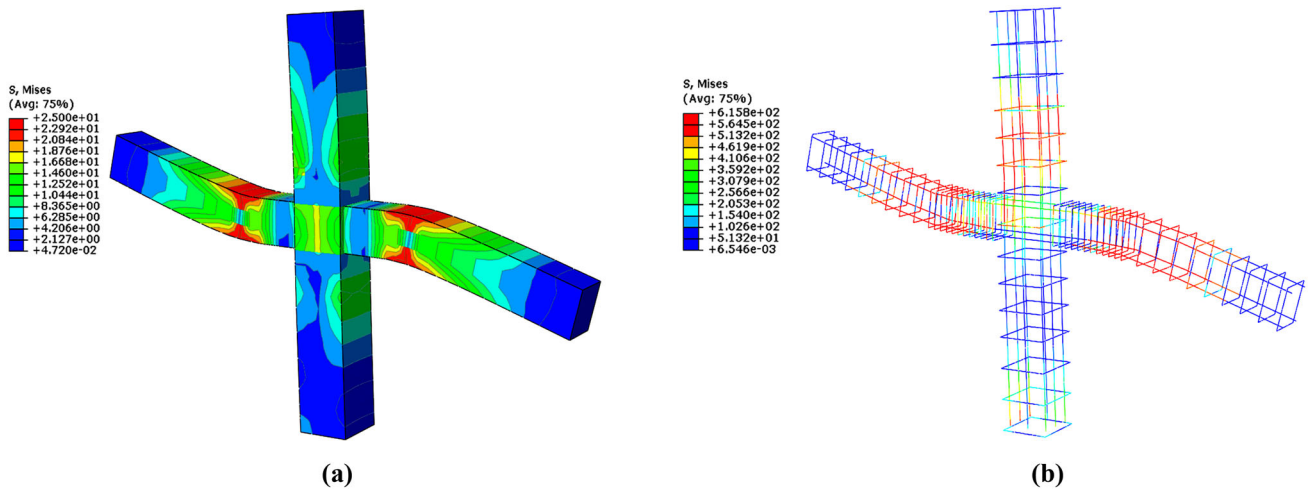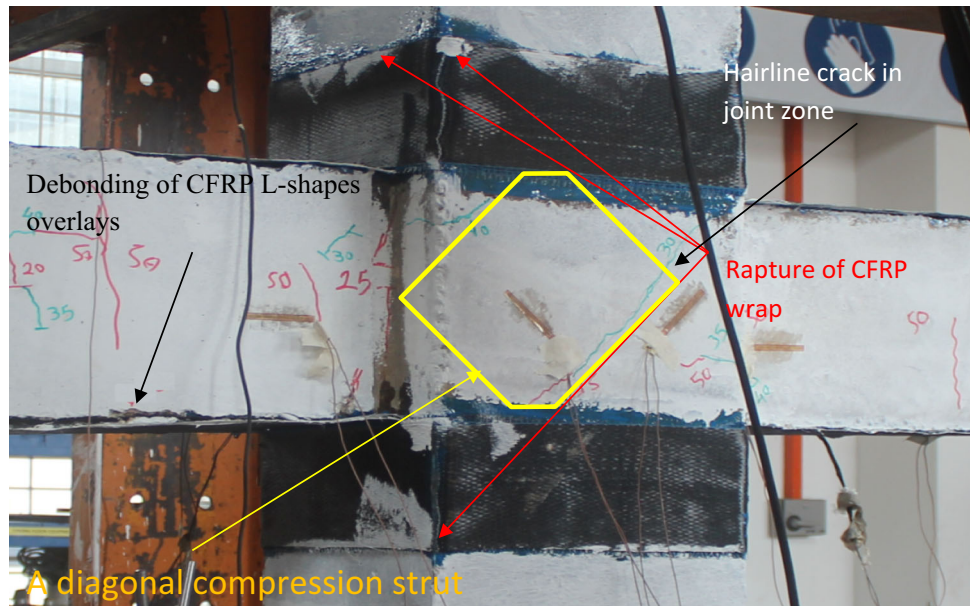
Fig. 18 Joint strengthened by CFRP modeled with ABAQUS software. **a** Concrete stress, **b** bar stress in joint strengthened by CFRP
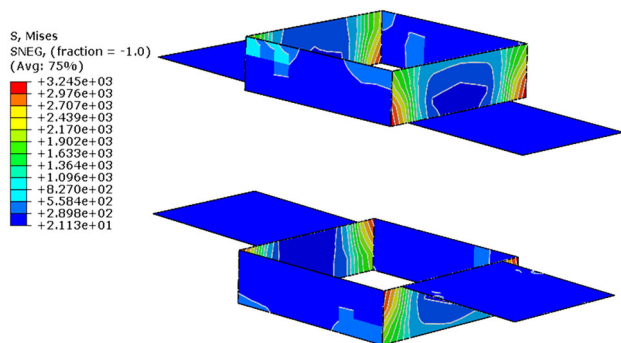
Fig. 19 Stress in the CFRP wrap and L-shape overlay

study, however, failure mechanism occurred in the beam region away from the joint region, which is clearly beneficial.

Fig. 20 Cracks paths of ABAQUS results in the joint tested by Esmaeeli et al. (2015)

4 Conclusion

The present study proposed a novel strengthening technique for beam–column joints. The experimental test achieved a basic understanding of the behavior of joint, strengthened by CFRP wrap, in columns region with L-shape overlays on the top and bottom of the beams. This system was to transfer the failure of the columns regions to the beams. Therefore, two interior beam–column joints were made and tested. One interior joint was tested in an unstrengthened condition to act as the control joint. The numerical simulation based on plastic damage model was conducted to study the behavior of joint, strengthened by CFRP sheets. It was noticed that debonding occurred between interfaces of the CFRP L-shapes overlay joint at failure load and rupture of the CFRP wrap. The results showed that the beam–column joint achieved higher ultimate force than control joint. The joint, strengthened by CFRP, was highly flexible, and the CFRP sheets dissipated the energy effectively. The result showed that the CFRP sheets could delay crack propagations and reduce the lengths of cracks in the joint region. The length of cracks decreased because CFRP sheets were applied. The average decrease was approximately 37% of the crack length of the control beam–column joint. It was found that the compression strut zone was increased by the application of CFRP wrap in the column zone.

Compliance with Ethical Standards

Conflict of interest The authors declare that there is no conflict of interest regarding the publication of this article.

References

Akguzel U, Pampanin S (2012) Assessment and design procedure for the seismic retrofit of reinforced concrete beam–column joints using FRP composite materials. J Compos Constr 16(1):21–34

Alhaddad M, Siddiqui N, Abadel A, Alsayed S, Al-Salloum Y (2012) Numerical investigations on the seismic behavior of FRP and TRM upgraded RC exterior beam–column joints. ASCE J Compos Constr 16(3):308–321

Baji H, Eslami A, Ronagh H (2015) Development of a nonlinear FE modelling approach for FRP-strengthened RC beam–column connections. Structures 3:272–285

Balaji S, Thirugnanam G (2017) Study on exterior RC beam–column joints upgrade with SIFCON in joint core under reversed cyclic loading. KSCE J Civ Eng 21(1):346–352

Bruno D, Greco F, Feudo S (2017) Edge debonding prediction in beams strengthened by FRP composite plates. Models Simul Exp Issues Struct Mech 8:105–124

Bsisu K, Hiari B (2015) Finite element analysis of retrofitting techniques for reinforced concrete beam–column joint. J Am Sci 11(8):48–56

Deaton JB (2013) Nonlinear finite element analysis of reinforced concrete exterior beam-column joints with nonseismic detailing. Doctoral dissertation, Georgia Institute of Technology

Del Vecchio C, Di Ludovico M, Balsamo A, Prota A, Manfredi G, Dolce M (2014) Experimental investigation of exterior RC beam–column joints retrofitted with FRP systems. J Compos Constr 18(4):1–13

Elshamandy M, Farghaly A, Benmokrane B (2018) Experimental behavior of glass fiber-reinforced polymer-reinforced concrete columns under lateral cyclic load. ACI Struct J 115(2):337–349

Esmaeeli E, Barros J, Sena-Cruz J, Fasan L, Prizzi F, Melo J et al (2015) Retrofitting of interior RC beam–column joints using CFRP strengthened SHCC: cast-in-place solution. Compos Struct 122:456–467

Nakaba K, Kanakubo K, Furuta T, Yoshizawa K (2001) Bond behavior between fiber reinforced polymer laminates and concrete. ACI Struct J 98:359–367

Rahimipour A, Hejazi F, Vaghei R, Jaafar M (2016) Finite element development of a beam–column connection with CFRP sheets subjected to monotonic and cyclic loading. Comput Concr Int J 18(6):083–1096

Realfonzo R, Napoli A, Pinilla J (2014) behavior of RC beam–column joints strengthened with FRP systems. Constr Build Mater 54:282–297

Santarsiero G (2018) FE modelling of the seismic behavior of wide beam–column joints strengthened with CFRP systems. Buildings 8(31):2–14

Shahbazpanahi S, Kamgar A (2014) A novel numerical model of debonding of FRP-plated concrete beam. J Chin Inst Eng 38:24–32

Shahbazpanahi S, Ali AA, Aznieta F, Kamgar A, Farzadnia N (2012) A simple method to model crack propagation in concrete. Constr J 13(1):41–50

Shahbazpanahi S, Ali AA, Aznieta FN, Kamgar A, Farzadnia N (2013a) A simple and practical model for FRP-reinforced cracked beam. Eur J Environ Civ Eng 18(3):293–306

Shahbazpanahi S, Ali AA, Aznieta FN, Kamgar A, Farzadnia N (2013b) Modelling of the fracture process zone to improve the crack propagation criterion in concrete. J S Afr Inst Civ Eng 55(3):2–9

Shahbazpanahi S, Abang A, Aznieta F, Kamgar A, Farzadnai N (2014a) A theoretical method for fracture resistance of shear strengthened RC beams with FRP. Arab J Sci Eng 39(5):3591–3597

Shahbazpanahi S, Abang A, Kamgar A, Farzadnia N (2014b) Fracture mechanic modeling of fiber reinforced polymer shear-strengthened reinforced concrete beam. Compos B 68:113–120

Shahbazpanahi S, Hejazi F, Paknahad M, Rahimipour A, Nassimi M (2018) Modeling crack propagation in RC beam–column joints. Tehnički Vjesnik - Technical Gazette **(in press)**

Singh V, Bansal PP, Kumar M, Kaushik S (2013) Experimental studies on strength and ductility of CFRP jacketed reinforced concrete beam–column joints. Constr Build Mater 55:194–201

Xiaobing S, Xianglin G, Yupeng L, Chang T, Weiping Z (2013) Mechanical behavior of FRP-strengthened concrete columns subjected to concentric and eccentric compression loading. J Compos Constr 17:336–346